Universal behaviors in granular flows and traffic flows

Hisao HAYAKAWA*) and Ken NAKANISHI*,**)

Graduate School of Human and Environmental Studies, Kyoto University, Kyoto 606-01, Japan

* *Department of Mechanical Engineering, Shizuoka University, Hamamatsu 432, Japan*

(Received November 8, 1997)

We review the current understanding on universal behaviors in granular flows through a vertical pipe and traffic flows. We carry out weakly nonlinear analysis of a model for traffic flows based on the technique of soliton perturbations, and determine the selected propagating velocity, the amplitude, the width of interfaces connecting between jam phase and non-jam phase. From the direct simulation of the model, we have confirmed the validity of our theoretical analysis. We also introduce a model for granular pipe flow supplemented by the white noise, which reproduces $P(f) \sim f^{-4/3}$, where $P(f)$ is the power spectrum in the frequency f. (This paper will be published in Progress of Thoeretical Physics Supplment).

§1. Introduction

Recently, cooperative dynamics in dissipative systems consisting of discrete elements have attracted much attention. Researches on granular materials are efforts to understand unusual behaviors of discrete element systems [1] such as convection [2], size segregation [3], bubbling [4], standing waves [5] and localized excitations [6] as well as thermodynamic descriptions of granular particles under the vertical vibrations [7]. In particular, it is interesting that jam formation of particles and a power law in the power spectra in flows of granular particles through a narrow vertical pipe. Similarly, traffic jams in a highway is also an attractive subject not only for engineers but for physicists [8]. Similarities between two phenomena are obvious. Both consists of discrete dissipative elements, vehicles and particles which are confined in a quasi one-dimensional systems such as a highway and a pipe. There is an optimal velocity in each system, the competition between the relaxation to the optimal velocity and acceleration of particles produces jam formation. We, thus, expect that there exists common and universal mathematical structure behind these phenomena.

In the next section, we will introduce typical models for granular flows and traffic flows, and summarize the current status of our understanding on universal properties in one-dimensional flows. Among these studies we will focus on recent two main streams in studies of granular flows and traffic flows. First, we will review the recent progress in theoretical analysis of pure one-dimensional models. The second, we will introduce the progress in analysis for power spectra in density auto-correlation function in quasi one-dimensional systems.

*) email: hisao@phys.h.kyoto-u.ac.jp

**) email: tmknaka@eng.shizuoka.ac.jp

From the theoretical analysis of pure one-dimensional models, at least, it has been confirmed that perturbed solitons by dissipative corrections play important roles in traffic flows and granular flows. In particular, Komatsu and Sasa [9] have revealed the mechanism of jam formation in a traffic flow by the perturbative treatment of solitons. Hayakawa and Nakanishi [10] have generalized the analysis of Komatsu and Sasa [9], and demonstrate that universal mathematical structure exists in pure one-dimensional models for granular flows and traffic flows. In section 3 consisting of three subsections, we will review the details of theoretical argument by Hayakawa and Nakanishi [10] which discussed a model of traffic flow. We will stress that the framework of our analysis can be used in any one-dimensional models for granular flows and traffic flows.

In realistic situations, however, e.g. highways have several lanes, and vehicles (particles) can pass slow vehicles (particles). When we include multi-lane effects in one-dimensional models, separations between jam and non-jam phases become obscured. However, there is another universal law in quasi one-dimensional systems for flows of dissipative discrete elements, i.e. a power law in power spectrum of density auto-correlation function of vehicles or particles. Recently, Moriyama et al. [11] have presented that the power spectrum is given by $P(f) \sim f^{-\alpha}$ with $\alpha \cong 1.33$ from their experiment on granular flow through a vertical pipe. This result is expected to be a universal in quasi one-dimensional dissipative flows such as traffic flows in a highway. Thus, we will clarify the mechanism to appear $f^{-4/3}$ law in section 4. For this purpose, we will introduce a simple model supplemented by the white noise. From the simulation of our model we will confirm that our model can reproduce $f^{-4/3}$. We will explain the mechanism how to obtain $f^{-4/3}$-law from the simple analytic calculation.

In section 5, we will give concluding remarks, especially on universality in granular flows through a pipe and traffic flows. We also summarize our results.

§2. Models

In this section let us summarize what models exist and what consensus in studies of granular flows and traffic flows is obtained.

There are many models to describe traffic flows and granular flows through a pipe. We believe that universal behaviors do not depend on the choice of the model. Recently, Hayakawa and Nakanishi [10] have proposed a generalized optimal velocity model for traffic flows

$$\ddot{x}_n = a[U(x_{n+1} - x_n)V(x_n - x_{n-1}) - \dot{x}_n], \tag{2·1}$$

where x_n and a are the positions of n th car, and the drag coefficient, respectively. This model contains the psychological effect of drivers. Namely, the driver of x_n takes care of not only the distance ahead $x_{n+1} - x_n$ but also the distance behind $x_n - x_{n-1}$. The optimal velocity function U should be a monotonic increasing function of the distance of $x_{n+1} - x_n$ and V should be a monotonic decreasing function of $x_n - x_{n-1}$.

Thus, we adopt

$$U(h) = \tanh(h-2) + \tanh(2); \quad V(h) = 1 + f_0(1 - \tanh(h-2)) \tag{2·2}$$

for the explicit calculation in section 3, where f_0 is a constant. We put these optimal velocity functions as the product form UV in (2·1), because the driver of x_n cannot accelerate the car without enough space ahead even when the distance $x_n - x_{n-1}$ becomes short. In other words, the model including $U(x_{n+1} - x_n) + V(x_n - x_{n-1})$ is mathematically unstable and unphysical, because the acceleration by V causes crash of vehicles. This model (2·1) with (2·2) is a generalization of the optimal velocity (OV) model proposed by Bando et al. [12)]

$$\ddot{x}_n = a[U(x_{n+1} - x_n) - \dot{x}_n]. \tag{2·3}$$

The generalized OV model is similar to the model of granular flow in a one-dimensional tube

$$\ddot{x}_n = \zeta[\tilde{U}(x_{n+1} - x_{n-1}) - \dot{x}_n] + T[\varphi'(x_{n+1} - x_n) - \varphi'(x_n - x_{n-1})], \tag{2·4}$$

where ζ and T are respectively the drag coefficient and the strength of collision among particles. $\tilde{U}$ and φ are the optimal velocity and soft core repulsion potential, respectively [11)].

There is a fluid field model to describe traffic flows [13)] which consists of mass conservation for density field ρ and momentum conservation for velocity field v as

$$\begin{aligned} \partial_t \rho &= -\partial_x(\rho v), \\ \partial_t v &= -v\partial_x v - \frac{T_e}{\rho}\partial_x \rho + \frac{U_\rho(\rho) - v}{\tau_\rho} + \frac{\eta}{\rho}\partial_x^2 v, \end{aligned} \tag{2·5}$$

where τ_ρ and T_e are a characteristic time for the relaxation and the effective temperature, respectively. This model also contains the relaxation mechanism to an optimal velocity U_ρ, while the pressure term and the viscous term are phenomenologically introduced to stabilize the solution of a set of equations (2·5).

This fluid model (2·5) is similar to fluid models to describe granular flows through a pipe and fluidized beds [14), 15), 16), 17)] and mixture of polymers [18)]. As a typical example, we write an explicit form of a fluid model for granular flow by Sasa and Hayakawa [15)] at the Froude number Fr:

$$\begin{aligned} \partial_t \rho &= -\partial_x(\rho v), \\ \partial_t v &= -v\partial_x v - \tilde{\zeta}(\rho)(V_0 - v) - \frac{1}{Fr} - f''(\rho)\partial_x \rho + \kappa \partial_x^3 \rho \\ &\quad + \frac{1}{\rho}\partial_x(\rho \nu(\rho)\partial_x v). \end{aligned} \tag{2·6}$$

Although this model seems to be complicated, each term corresponds to that in eq.(2·5). Here the term in proportion to κ is introduced to stabilize the solution furthermore, which can be regarded as a coupling term in mixing free energy. The pressure $f'(\rho)$ arises from the collisions among particles, which is a recovery force to

the mean density ρ_0 and diverges at the closest packing states at ρ_{cp}. The kinetic viscosity $\nu(\rho)$ also diverges at ρ_{cp}. Komatsu and Hayakawa [16], thus, adopted $f(\rho) = \beta_1(\rho - \rho_0)^2/(\rho_{cp} - \rho)$ and $\nu(\rho) = \beta_2/(\rho_{cp} - \rho)$ for the simulation of (2·6), where β_1 and β_2 are constants. The optimal velocity V_0 is assumed to be a constant because of the incompressibility of the fluid, and $\tilde{\zeta}(\rho)$ is a phenomenological function to be determined by the sedimentation rate.

At first sight fluid models (2·5) and (2·6) are very different from discrete models such as (2·1), (2·3) and (2·4). However, there is common mathematical structure. The fluid models of granular flows such as eq.(2·6) are reduced to the Korteweg-de Vries (KdV) equation near the neutral curve of the linear stability [15), 16), 17)]. Kurtze and Hong [19)] also derived KdV equation from the fluid model of the traffic flow (2·5) [13)]. Of course, it is easy to derive KdV equation from the discrete models (2·1), (2·3) and (2·4) near the neutral curve. Thus, at least, we get a consensus that dissipative solitons play important roles for granular flows and traffic flows.

Unfortunately KdV equation is not adequate to describe the traffic jams, because solutions of these equations are essentially pulses and no interface solutions connecting jam phase with non-jam phase are included. Komatsu and Sasa [9)] solved such a puzzle from the analysis of the original OV model (2·3). They have showed that (2·3) can be reduced to the modified KdV (MKdV) equation at the critical point (the averaged car distance $h = 2$) or the most unstable point on the neutral curve. They also show that symmetric kink solitons deformed by dissipative corrections describe a phase separation between bistable phases. This analysis is also consistent with recent analysis for the exactly solvable models which may be regarded as simplified optimal velocity models [20)]. However, as will be shown, the generalized optimal velocity model (2·1) and granular model (2·4) as well as the fluid model (2·5) of traffic flows [13)] and fluid models, e.g. (2·6) for granular flows [15), 16), 17)] are not reduced to MKdV equation at the critical point or the most unstable point on the neutral curve. In fact, Komatsu [21)] has shown that the fluid model (2·5) has the following properties: (i) Interfaces (kinks) between jam and non-jam phases are asymmetric. (ii) The critical point to appear kinks is, in general, different from the most unstable point on the neutral curve. (iii) Eventually one branch of the coexistence curve exists in the linearly unstable region. He also demonstrates that MKdV equation is recovered in a special choice of parameters of the fluid model, while fluid models cannot be reduced to MKdV equation in general cases. Thus, we need to clarify universal characteristics of dissipative particle dynamics in general cases which contains (2·1), (2·4) and fluid models [13), 14), 15), 16), 17)]. For this purpose, we will focus on analysis the simplest model (2·1) among them to characterize the phase separation between jam and non-jam phases.

We may be suspicious of reality and relevancy of pure one-dimensional models. As indicated in Introduction, when we include multi-lane effects in one-dimensional models, separations between jam and non-jam phases become obscured. However, the fundamental characteristics of pure one-dimensional models should be important for quasi one-dimensional cases. To demonstrate the relevancy of pure one-dimensional models, we will focus on another universal law in quasi one-dimensional systems, i.e. a power law in power spectrum of density auto-correlation function of

vehicles or particles.

Power-law form of the power spectrum $P(f) \sim f^{-\alpha}$, where f is frequency, of density fluctuations was found in both numerical simulations [22] and experiments [23), 24]. Although their interpretations on the origin of the emergence of density waves are different, estimated values of the exponent α is close to each other ($1.3 < \alpha < 1.5$). The previous reports [23), 24] on the estimation $\alpha \cong 1.5$ seem a little ambiguous: The volume of air flow out of the bottom end of the pipe was not well controlled. Besides, the power spectra they obtained were still noisy. Recently, Moriyama et al. [11] have presented better-controlled air flow out of the pipe and more accurate experimental results than the previous ones by increasing the number of trials. One of their results is the precise estimation of the scaling exponent of the power spectrum $P(f) \sim f^{-\alpha}$ with $\alpha \cong 1.33$. This result is identical to that by LGA [22], and is expected to be a universal law in quasi one-dimensional dissipative flows such as traffic flows in a highway.

The second purpose of this paper is to clarify the mechanism to appear $f^{-4/3}$ law in power spectra. We, thus, extend the one-dimensional model (2·4) to a stochastic model supplemented by the white noise as

$$\begin{aligned} \ddot{h}_n = \zeta[\tilde{U}(\frac{h_{n+1}+h_n}{2}) - \tilde{U}(\frac{h_n+h_{n-1}}{2})] - \dot{h}_n] \\ +T[\varphi'(h_{n+1}) + \varphi'(h_{n-1}) - 2\varphi'(h_n)] + f_n(t), \end{aligned} \tag{2·7}$$

where $h_n = x_{n+1} - x_n$. The most crucial simplification of the model is that f_n is assumed to be the Gaussian white noise with zero mean. The optimal velocity $\tilde{U}(h)$ may be the sedimentation rate which is a function of the local volume fraction [25] in general. It should be noticed that the drag ζ is irrelevant in systems where the bottom end of the pipe is fully open, because air in the pipe flows away together with particles. Thus, to observe density waves it is important to close the cock of the pipe.

One of the important points is that the white noise is introduced not to an equation for x_n but to an equation for the relative motion of particles h_n, because the ordering of particles along a pipe or a highway is not conserved due to passing of particles in multi-lane or multi-dimensional systems. From both simulation and analytic calculation of (2·7), we will demonstrate that this simple model reproduces $\alpha = 4/3$ near the neutral curve of the linear stability analysis of uniform states in section 3. We can expect the existence of a universal law regardless to the choice of a specific model. Therefore, the model (2·1) for h_n supplemented by the white noise is expected to belong to the same universality class that by (2·7). The fluid models (2·5) and (2·6) with non-conserved white noise also should behave similarly as those for discrete models.

Now, we have come back to an interesting question: What are good models among many models? The answer is simple. The simple models are good ones. For example, when we compare discrete models (2·1) and (2·4) with fluid models (2·5) and (2·6), the representation of discrete models are shorter than fluid models. Since fluid models are partial differential equations, we may need careful check of the validity of the simulation scheme and long CPU time to simulate them. On the

other hand, discrete models which are coupled ordinary differential equations are free from such problems. The theoretical analysis for discrete models is also simpler than that for fluid models, because each discrete model contains only one set of equations. On the other hand, eq.(2·3) is a oversimplified model which loses some of universal properties. Therefore, we believe that models (2·1) and (2·4) are the most fundamental ones. In the following sections, thus, we will focus on the analysis of discrete models (2·1) and (2·7).

§3. Theory of a pure one dimensional model for traffic flow

In this section, we concentrate on the analysis of (2·1). The result explained in this section is universal for all of models introduced in the previous section. This section consists of three subsections. In the first subsection, we will summarize the result of linear stability analysis for uniform flows. In the next subsection, the main part of this section, the details of weakly nonlinear analysis will be explained, where a steady propagating solution is presented and the selection of its propagating velocity, the width of interfaces and the amplitude will be discussed. In the last subsection, we will confirm the validity of our theoretical analysis from the comparison between direct simulation and theoretical results.

3.1. *Linear stability of uniform flow*

In this subsection we summarize the linear stability analysis of the uniform propagating flow.

It is obvious that there is a constant propagating solution with $x_{n+1} - x_n = constant$. Let us rewrite (2·1) as

$$\ddot{r}_n = a[U(h + r_{n+1})V(h + r_n) - U(h + r_n)V(h + r_{n-1}) - \dot{r}_n], \tag{3·1}$$

where h is the averaged distance of successive cars and r_n is $x_{n+1} - x_n - h$. The linearized equation of (3·1) around $r_n(t) = 0$ is given by

$$\ddot{r}_n = a[U'(h)V(h)(r_{n+1} - r_n) + U(h)V'(h)(r_n - r_{n-1}) - \dot{r}_n], \tag{3·2}$$

where the prime refers to the differentiation with respect to the argument. With the aid of the Fourier transform

$$r_q(t) = \frac{1}{N}\sum_{n=1}^{N} \exp[-iqnh]r_n(t) \tag{3·3}$$

with $q = 2\pi m/Nh$ and the total number of cars N we can rewrite (3·2) as

$$(\partial_t - \sigma_+(q))(\partial_t - \sigma_-(q))r_q(t) = 0 \tag{3·4}$$

with

$$\sigma_\pm(q) = -\frac{a}{2} \pm \sqrt{(a/2)^2 - aD_h[U,V](1 - \cos(qh)) + ia(UV)'\sin(qh)}, \tag{3·5}$$

where we drop the argument h in U and V. $D_h[U,V] \equiv U'(h)V(h) - U(h)V'(h)$ denotes Hirota's derivative. The solution of the initial value problem in (3·4) is the

linear combination of terms in proportion to $\exp[\sigma_+(q)t]$ and $\exp[\sigma_-(q)t]$. The mode in proportion to $\exp[\sigma_-(q)t]$ can be interpreted as the fast decaying mode, while the term in proportion to $\exp[\sigma_+(q)t]$ is the slow and more important mode.

The violation of the linear stability of the uniform solution in (3·2) is equivalent to $Re[\sigma_+(q)] \geq 0$. Assuming $qh \neq 0$ ($qh = 0$ is the neutral mode), the instability condition is given by

$$2(UV)'^2 \cos^2(\frac{qh}{2}) \geq aD_h[U,V]. \tag{3·6}$$

Thus, the most unstable mode exists at $qh \to 0$ and the neutral curve for long wave instability is given by

$$a = a_n(h) \equiv \frac{2(UV)'^2}{D_h[U,V]}. \tag{3·7}$$

The neutral curve in the parameter space (a,h) is shown in Fig.1 for $f_0 = 1/(1+\tanh(2))$ in (2·2). For later convenience, we write the explicit form of the long wave expansion of σ_+ in the vicinity of the neutral curve

$$\sigma_+(q) = ic_0qh - c_0^2\frac{a-a_n(h)}{a_n(h)^2}(qh)^2 - i\frac{(qh)^3}{6}c_0 - \frac{(qh)^4}{4a_n(h)}c_0^2 + O((qh)^5), \tag{3·8}$$

where $c_0 = (UV)'$. Thus, the uniform state becomes unstable due to the negative diffusion constant for $a < a_n(h)$.

3.2. *Nonlinear analysis*

The simplest way to describe nonlinear dynamics is the long wave expansion with the help of a suitable scaling ansatz. It is easy to derive the KdV equation near the neutral curve from (2·1) as in the case of fluid models [15), 16), 17), 19)]. As mentioned in Introduction, to describe the phase separations, however, we should choose the critical point $(a,h) = (a_c, h_c)$ at $(U(h)V(h))'' = 0$ where the coefficient of $\partial_x r^2$ becomes zero on the neutral curve. At this point the cubic nonlinear terms can produce the interface solution to connect two separated domains. The explicit critical point of (2·2) with $f_0 = 1/(1+\tanh(2))$ is given by

$$h_c = 2 - \tanh^{-1}(1/3) \simeq 1.65343; \quad a_c = \frac{512}{81}f_0^2 \simeq 1.63866. \tag{3·9}$$

Unfortunately, the reduced equation based on the long wave expansion of our model is an ill-posed equation. In fact, the scaling of variables as $r_n(t) = \epsilon r(z,\tau)$, $z = \epsilon(n + c_0 t)$ and $\tau = \epsilon^3 t$ with $\epsilon = \sqrt{(a_c - a)/a_c}$ leads to

$$\partial_\tau r = a_1\partial_z r^3 - a_2\partial_z^3 r + a_3\partial_z^2 r^2 \tag{3·10}$$

in the lowest order, where a_1, a_2 and a_3 are constants. The solution of (3·10) is blown up within finite time. The reason is simple. Its linearized equation around $r = d_0$ is unstable for all scale, because the solution with $r - d_0 \simeq \exp[ikz + \lambda_k\tau]$ has the growth rate $Re[\lambda_k] = 2k^2 a_3 d_0$ which is always positive when $a_3 d_0 > 0$. Therefore, the simple long wave expansion adopted by Komatsu and Sasa [9)] for (2·3) and $a_3 = 0$ cannot be used in our case.

This short scale instability in (3·10) arises from the long wave expansion. To avoid such the difficulty, we only focus on a steady propagating solution for the theoretical analysis. Dynamical behavior is followed by the direct simulation of discrete model (2·1), where simulation of (2·1) is much easier than that of the reduced partial differential equations such as MKdV. In addition, our long time simulation suggests that the solution of (2·1) seems to be relaxed to a steady propagating mode.

To obtain the steady propagating kink solution, at first we eliminate the fast decaying mode in (3·1) as

$$(\partial_t - \sigma_+(\partial_x))r(x,t) = (\sigma_+ - \sigma_-)^{-1} N[r(x,t)], \tag{3·11}$$

where $N[r]$ represents the nonlinear terms

$$\begin{aligned}\frac{N[r]}{a} &= U(h+e^{h\partial_x}r)V(h+r) - U(h+r)V(h+e^{-h\partial_x}r) \\ &\quad -U'(h)V(h)(e^{h\partial_x}-1)r(x,t) + U(h)V'(h)(1-e^{-h\partial_x})r(x,t). \end{aligned}\tag{3·12}$$

Since $(\sigma_+ - \sigma_-)^{-1}$ is the inverse of the polynomial of the differential operators, it is convenient to use the expansion $(\sigma_+ - \sigma_-)^{-1} \simeq a^{-1}[1 - \frac{2h}{a}(UV)'\partial_x + O(h^2)]$. It should be noticed that (3·11) contains most of important information and no instability in time evolution.

To obtain the scaled propagating kink solution we assume the scaling of the variables by $\epsilon = \sqrt{(a_c - a)/a_c}$ as

$$r(x,t) = \epsilon\sqrt{\frac{6\gamma c_0}{|(UV)'''|}}R(z): \quad z = \epsilon\sqrt{6\gamma}(n + c_0 t - \epsilon^2\gamma(t)t), \tag{3·13}$$

where the arguments in U and V are fixed at $h = h_c$, and γ is the positive free parameter which will be determined from the perturbation analysis. The expansion of $N[r]$ is given by

$$N[r]/a = \sum_{n=1}^{\infty}\sum_{m=2}^{\infty} h^m C_{mn}\partial_x^n r^m - h^3 U'V'\partial_x r\partial_x^2 r + \cdots, \tag{3·14}$$

where $C_{21} = \frac{1}{2}(UV)'', C_{22} = \frac{1}{4}D_h[U,V]', C_{23} = \frac{1}{12}(UV)'', C_{31} = \frac{1}{6}(UV)''', C_{32} = \frac{1}{12}D_h[U,V]'', C_{41} = \frac{1}{24}(UV)''''$ with $D_h[U,V]' = \dfrac{d}{dh}D_h[U,V]$. Substituting (3·13) into (3·11) with the help of (3·14) we obtain

$$\frac{d}{dz}\left\{\frac{d^2R}{dz^2} - R(R^2-1) + \beta\frac{d}{dz}(R^2)\right\} = \epsilon\frac{d}{dz}M[R], \tag{3·15}$$

where $\beta = 3D_h[U,V]'/(2\sqrt{c_0|(UV)'''|})$ and

$$M[R] = \sqrt{\gamma}[\rho_{23}\left(\frac{dR}{dz}\right)^2 - \rho_{32}\frac{dR^3}{dz} - \rho_{41}R^4 - \frac{1}{4\eta}(4\frac{dR}{dz} + \frac{d^3R}{dz^3} - \frac{2}{\gamma}\frac{dR}{dz})] + \dot{\gamma}[\frac{zR}{2\gamma^{5/2}} - \gamma t R]. \tag{3·16}$$

Here $\dot{\gamma} = d\gamma/d\tau$ with $\tau = \epsilon t$, and $1/\eta = \sqrt{6}D_h[U,V]/c_0$, $\rho_{23} = 3\sqrt{6}U'V'/\sqrt{c_0|(UV)'''|}$, $\rho_{32} = \sqrt{3/2}D_h[U,V]''/|(UV)'''|$ and $\rho_{41} = \sqrt{3c_0}(UV)''''/(2\sqrt{2|(UV)'''|^3})$.

Assuming $R(z) = R_0(z) + \epsilon R_1(z) + \cdots$, we obtain a solution

$$R_0^{(\pm)}(z) = \tanh(\theta_\pm z); \quad \theta_\pm = \frac{\beta \pm \sqrt{\beta^2+2}}{2} \tag{3·17}$$

in the lowest order. This solution represents a kink or an anti-kink connecting between jam and non-jam phases because of $\theta_+ > 0$ and $\theta_- < 0$. Notice that the solution is not localized one and does not satisfy the periodic boundary condition. Therefore, we need a careful treatment of the boundary condition. In fact, our preliminary result [26] suggests that the selected value of γ under the open boundary condition is different from that under the periodic boundary condition.

In this paper we restrict ourselves to the case under the periodic boundary. To satisfy the periodic boundary condition, we use

$$R_0(z) \simeq {R_0}^{(+)}(z - z_+) - 1 + {R_0}^{(-)}(z - z_-) \tag{3·18}$$

as an approximate solution of the lowest order equation (3·15), where a pair of kink and anti-kink exists at $z = z_+$ and $z = z_-$. Since (3·18) is not an exact solution of (3·15), there should be an interaction between the kink and the anti-kink which is an exponential function of the distance between them [26].

Now, let us discuss the effect of perturbative terms in (3·15). It is known that perturbation of solitons or solution including a free parameter becomes unstable except for the solution where the parameter has a special value. [9),27),28),29),30),31),32)]. The linearized equation of (3·15) can be reduced to

$$\mathcal{L}R_1 = \frac{d}{dz}M[R_0], \tag{3·19}$$

where

$$\mathcal{L} = \partial_z^3 + \partial_z - 6R_0\partial_z - 3R_0^2\partial_z + 2\beta\partial_z^2 R_0 + 4\beta\partial_z R_0\partial_z + 2\beta R_0\partial_z^2. \tag{3·20}$$

To obtain a regular behavior of perturbation in $O(\epsilon)$ the perturbed solution should satisfy the solvability condition

$$(\Psi_0, \frac{d}{dz}M[R_0]) \equiv \lim_{L\to\infty}\int_{-L}^{L} dz\Psi_0\frac{d}{dz}M[R_0] = 0, \tag{3·21}$$

where L is the system size and Ψ_0 satisfies

$$\mathcal{L}^\dagger\Psi_0 = 0: \quad \mathcal{L}^\dagger = -\partial_z^3 - \partial_z + 3R_0^2\partial_z + 2\beta R_0\partial_z^2. \tag{3·22}$$

When we adopt (3·18) as R_0, Ψ_0 also should satisfies the periodic boundary condition. Thus, we assume

$$\Psi_0(z) = {\Psi_0}^{(+)}(z - z_+) - 1 + {\Psi_0}^{(-)}(z - z_-), \tag{3·23}$$

where $\Psi_0^{(\pm)}$ is the solution of (3·22) when we replace R_0 by $R_0^{(\pm)}$. Since $\Phi_0 \equiv \partial_z\Psi_0$ satisfies

$$\tilde{\mathcal{L}}^\dagger\Phi_0(z) = 0; \quad \tilde{\mathcal{L}}^\dagger = -\partial_z^2 - 1 + 3R_0^2 + 2\beta R_0\partial_z, \tag{3·24}$$

the solution of (3·22) can be expressed by

$$\Psi_0{}^{(\pm)}(z) = \frac{\alpha_\pm}{2}\int_{-z}^{z} dz'(\mathrm{sech}[\theta_\pm z'])^{1/\theta_\pm^2}; \quad \Psi_0^{(\pm)}(z) = -\Psi_0^{(\pm)}(-z), \tag{3·25}$$

where we use

$$\Phi_0^{(\pm)}(z) = (\mathrm{sech}[\theta_\pm z])^{1/\theta_\pm^2}. \tag{3·26}$$

The constant $\alpha_\pm$ in (3·25) is determined to satisfy $\Psi_0(\pm\infty) = -1$. Thus, we obtain

$$\alpha_\pm = \frac{2\theta_\pm}{I_0{}^{(\pm)}}; \quad I_n^{(\pm)} = \int_{-\infty}^{\infty} dx(\mathrm{sech}x)^{1/\theta_\pm^2+2n} = \sqrt{\pi}\frac{\Gamma(1/(2\theta_\pm^2)+n)}{\Gamma(1/(2\theta_\pm^2)+n+1/2)}, \tag{3·27}$$

where $\Gamma(x)$ is the gamma function. It should be noticed that $\Psi_0(z)$ is not a localized function. Therefore, we cannot neglect the boundary effects in the solvability condition (3·21).

Let us rewrite (3·21) as

$$[\Psi_0 M[R_0]]_{-L}^{L} = (\Phi_0(z), M[R_0]), \tag{3·28}$$

where $[f(z)]_{-L}^{L} = f(L) - f(-L)$. From (3·16) it is obvious that contribution from terms except for those in proportion to ρ_{41} and zR is zero in the left hand side of (3·28) under any boundary conditions. Notice that the contribution from the term in proportion to tR vanishes because of its symmetry. If we adopt the periodic boundary condition and use (3·18) and (3·23), the contribution from the term ρ_{41} is canceled [33]. Thus, the left hand side of (3·28) is reduced to

$$[\Psi_0 M[R_0]]_{-L}^{L} = \frac{\dot\gamma}{\gamma^{5/2}}L. \tag{3·29}$$

On the other hand, the right hand side of (3·28) is the integration of the product of (3·16) and (3·26).

For simplicity, to obtain the explicit form we assume $f_0 = 1/(1+\tanh(2))$ in (2·2). In this case the coefficients in (3·31) are reduced to $\rho_{23} = -3/2$, $\rho_{32} = -\beta$, $\rho_{41} = -1/4$, $\eta = 1/(4\beta)$ $c_0 = 2^6 f_0/3^3 = 1.20689$, and $\beta = 3\sqrt{3}/(8\sqrt{2}f_0) = 0.902037$, $6c_0/|(UV)'''| = 9/4$, $\theta_+ = 1.2897187$, $\theta_- = -0.387814$. Finally we obtain

$$\{L - (\theta_+ - \theta_-)\}\dot\gamma = 4\beta\gamma^2\{\frac{\theta_+}{\theta_+^2+1}(1-\frac{\gamma}{\gamma_+}) - \frac{\theta_-}{\theta_-^2+1}(1-\frac{\gamma}{\gamma_-})\}, \tag{3·30}$$

where we use $\dfrac{I_{n+1}^{(\pm)}}{I_n^{(\pm)}} = \dfrac{2n\theta_\pm^2+1}{(2n+1)\theta_\pm^2+1}$. Here $\gamma_\pm$ is given by

$$\begin{aligned}\gamma_\pm^{-1} = {} & 2 + \theta_\pm^2\left(2 - 3\frac{I_2^{(\pm)}}{I_1^{(\pm)}}\right) \\ & +2\eta[3\rho_{32}\left(1-\frac{I_2^{(\pm)}}{I_1^{(\pm)}}\right) + \frac{\rho_{41}}{\theta_\pm}\left(\frac{I_0^{(\pm)}}{I_1^{(\pm)}} - 2 + \frac{I_2^{(\pm)}}{I_1^{(\pm)}}\right) - \rho_{23}\theta_\pm\frac{I_2^{(\pm)}}{I_1^{(\pm)}}].\end{aligned} \tag{3·31}$$

Thus, we obtain $\gamma_\pm$ as

$$\gamma_\pm = \frac{8\beta\theta_\pm(3\theta_\pm^2+1)}{37\theta_\pm^4+8\theta_\pm^2-8}. \tag{3·32}$$

Substituting (3·32) into (3·30) we obtain

$$(L-\theta_++\theta_-)\dot{\gamma} = \alpha\gamma^2(1-\frac{\gamma}{\gamma^*}), \tag{3·33}$$

where

$$\alpha = \frac{24\beta\sqrt{\beta^2+2}}{4\beta^2+9}; \quad \gamma^* = \frac{3(12\beta^2+25)}{61\beta^2+132} = 0.574189\cdots. \tag{3·34}$$

From (3·13) the amplitude $A\epsilon$ of R_0 can be regarded as the order parameter of phase separation, which is given by

$$A\epsilon \equiv \frac{3}{2}\epsilon\sqrt{\gamma^*} = 1.13663\epsilon. \tag{3·35}$$

In the vicinity of γ^* the time evolution of γ is described by

$$\gamma(\tau) \simeq \gamma^* + A\exp[-\frac{\alpha\gamma^*}{L}\tau] \tag{3·36}$$

Notice that γ^* is the stable fixed point in the time evolution (3·33). where we use $\dfrac{\theta_+-\theta_-}{L} \ll 1$.

Two remarks on the result of this section are addressed: We recall that to derive (3·34) from (3·28) we assume $f_0 = 1/(1+\tanh(2))$. Although to obtain the result for any f_0 is not difficult, we omit such a generalization to avoid long and tedious calculations. Thus, the expression with $\beta = 0$ in (3·34) does not recover the result by Komatsu and Sasa [9]. As the second remark, the characteristic time for the relaxation (3·33) or (3·36) is proportional to the system size L. This result is reasonable, because the time needed to simulate (2·1) is proportional to number of cars N. This tendency has been confirmed by our simulation.

3.3. *Simulation*

To check the validity of our analysis in the previous subsection we perform the numerical simulation of (2·1) and (2·2) with $f_0 = 1/(1+\tanh(2))$ near the critical point (3·9) under the periodic boundary condition. We adopt the classical fourth-order Runge-Kutta scheme with fixed time interval $\Delta t = 2^{-4}$. Since our purpose is the quantitative test of (3·17) and (3·34), the initial condition is restricted to the localized symmetric form $r_n = 18.7/N(\tanh(n-N/4)-\tanh(n-3N/4)-1)$ where N is the number of cars. Taking into account the scaling properties we perform the simulation for the set of parameters $(\epsilon, N) = (1/2, 32), (1/4, 64), (1/8, 128), (1/16, 256)$ until r_n relaxes to a steady propagating state. Our results are plotted in Figs.1 and 2.

Figure 1 displays points which have the maximum h_{max} and the minimum h_{min} values of successive car distance in each parameter set, and theoretical coexistence

curve

$$a = a_c \left(1 - \frac{(h - h_c)^2}{A^2} \right); \quad A = 1.13663 \cdots, \tag{3·37}$$

where we use $a = a_c(1 - \epsilon^2)$ and $A\epsilon = h - h_c$. The agreement with each other is obvious. From this figure we can see that one of the branches is in the linearly unstable region but the theoretical curve recovers the simulation result. We stress that the evaluated value of A from simulation at $\epsilon = 1/16$ is $1.14273 \cdots$. Thus, the deviation between simulation and theory is only 0.53 %.

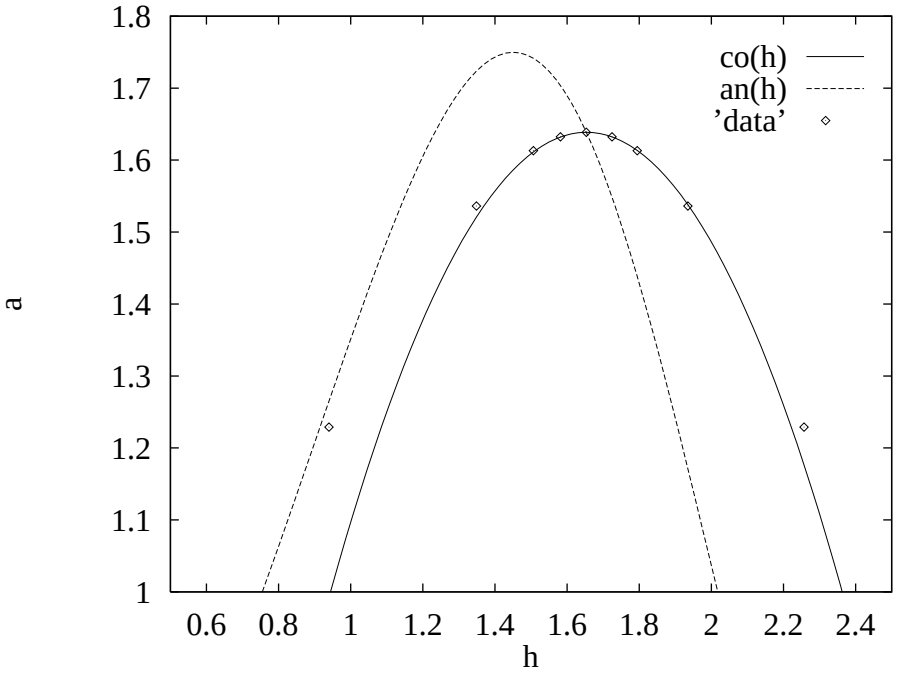

Fig. 1. Theoretical coexistence curve (solid line) $a = a_c(1 - (h - h_c)^2/A^2)$ where $A = 1.13663$, $h_c = 1.65343$ and $a_c = 1.63866$, and the neutral curve (broken line) for the model described by eq.(2) with $W(h) = \tanh(h - 2) + \tanh(2)$, $V(h) = 1 + (1 - \tanh(h - 2))/(1 + \tanh(2))$ and $f_n = 0$. h denotes the average distance between successive cars. The data is obtained for minimum and maximum values of r_n at a given a.[10)]

Figure 2 demonstrates that the numerical result has a scaling solution which has an asymmetric kink-antikink pair. The linear combination of our theoretical curve (3·17) with (3·32) is plotted as the solid line by choosing the position of the kink and the anti-kink. Our theoretical curve agrees with the result of our simulation without other fitting parameters. Thus, we have confirmed the validity of our theoretical analysis.

§4. $f^{-4/3}$ law in power spectra

The purpose of this section is to clarify the mechanism to appear $P(f) \sim f^{-4/3}$ law in power spectra. We, thus, extend the one-dimensional model (2·4) to a stochas-

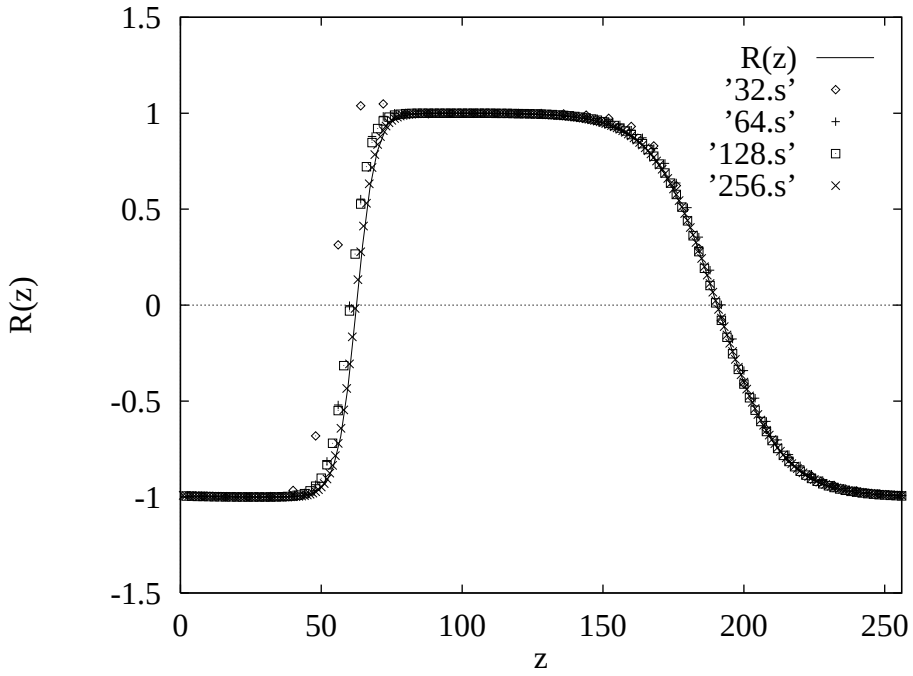

Fig. 2. Theoretical curve (solid line) and scaled data obtained from our simulation for scaled r_n. Each data denotes $(\epsilon, N) = (1/2, 32), (1/4, 64), (1/8, 128), (1/16, 256)$, where $\epsilon = (1 - a/a_c)^{1/2}$, $'N.s'$ represents the data for N cars (particles). Theoretical curve is given by $R(z) = \tanh(\xi\theta_+(z-z_+))-1+\tanh(\xi\theta_-(z-z_-))$ with $\xi = (6\gamma^*)^{1/2}/16$, $\gamma^* = 0.574189$, $\theta_+ = 1.2897187$ and $\theta_- = -0.3876814$, where only $z_+ = 62.5$ and $z_- = 190.5$ are fitting parameters. Spatial scale is measured by the scale for $N = 256$.[10)]

tic model (2·7) supplemented by the white noise. We will demonstrate the simple model reproduces $\alpha = 4/3$ near the neutral curve of the linear stability analysis of uniform states.

At first, we briefly summarize the result of linear stability. Although the framework is common with that in section 3.1, the explicit forms are a little different. The neutral curve is given by $T_n = \tilde{U}'^2/\varphi''(h)$. The critical point is given by the cross point of $\tilde{U}''(h_c) = 0$ on the neutral curve. We will focus on the behaviors for weakly unstable or stable region at $T = T_c(1 - \mu)$ with $|\mu| \ll 1$.

Let us simulate (2·7) directly. Adopting

$$\tilde{U}(r) = \tanh(r - 2) + \tanh(2), \quad \varphi(r) = \mathrm{sech}^2(r) \tag{4·1}$$

with $\zeta = 2$, $N = 256$, $T_c = 3.95798\cdots$, and $h = 2$ at $t = 0$, we numerically calculate (2·7) by the classical Runge-Kutta method until $t = 2^{11}$ with time interval $\Delta t = 1/2^4$ under the periodic boundary condition. We use the uniform random number distributed between $-X$ and X with $X = 9/1024$ for $f_n(t)$. Figure 3 displays the power spectrum $P(f) =< |\tilde{\rho}(f)|^2 >$ obtained from our simulation of (2·7) at $\mu = 1/64$, where $\tilde{\rho}(f)$ is the Fourier transform of the discretely sampled data of the density $\rho(t) = \dfrac{1}{N}\displaystyle\sum_n \frac{1}{r_n(t)}$ with the time interval 1. This clearly supports $P(f) \sim f^{-4/3}$ law

in the range of f between 10 and 1000 as in the experiment [11]. It should be noticed that the data in Fig.3 may suggest steeper slope than $f^{-4/3}$ in low frequency region $f < 10$. Although the steep slope close to $f^{-3/2}$ at small f is not observed in the experiment by Moriyama et al. [11], it can be explained easily by the diffusive behavior of an interactive pair of kink and antikink. The details of the process to produce $f^{-3/2}$ will be reported elsewhere.

From the examinations of several values of μ, we have confirmed that the qualitative results are insensitive to the sign of μ when $|\mu| \ll 1$. This result is reasonable because near the neutral curve the time scale of relaxation or growth of fluctuations is much longer than the time scale induced by the noise $f_n(t)$. Our numerical result suggests that the linear relaxation theory of fluctuations can be used to explain $P(f) \sim f^{-4/3}$. This $f^{-4/3}$ law can been seen from the simulation of traffic flow (2·1) with the noise.

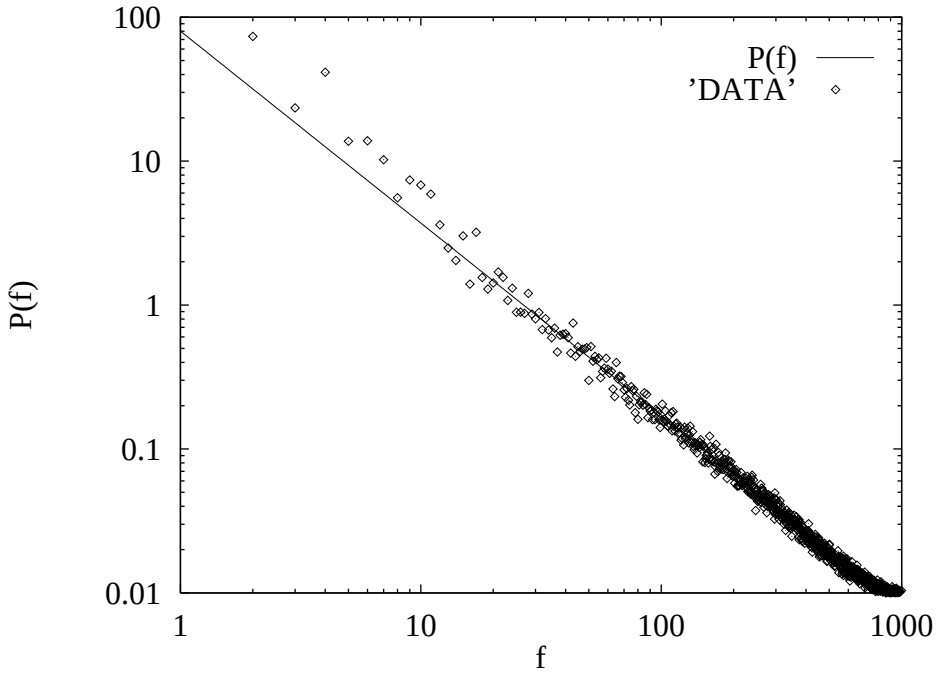

Fig. 3. Log-log plot of power spectrum $P(f)$ obtained from the simulation of eq.(2.7) with (4.1), where the unit of f is $1/(2\pi)$ and the unit of $P(f)$ is not normalized. The solid line represents $f^{-4/3}$.

Thus, let us briefly explain how to appear $f^{-4/3}$ law from the behavior of structure factor

$$S_k(t) \equiv \sum_{n,m} < \exp[ik(r_n(t) - r_m(0))] >= \frac{1}{N} \sum_{n,m} \exp\left[-\frac{k^2}{2}\phi_{nm}(t)\right], \qquad (4\cdot2)$$

where $\phi_{nm}(t) =< (r_n(t) - r_m(0))^2 >$. Notice that the structure factor is directly related to the auto-correlation function as $S_k(t) = \int_0^t dt' < \rho_k(t+t')\rho_{-k}(t) >$, where $\rho_k(t)$ is the Fourier component of the density field of particles $\rho(\mathbf{r}, t)$. In weakly stable

states, *i.e.* $\mu < 0$ and $|\mu| \ll 1$, $S_k(t)$ can be calculated as in the case of polymer dynamics [34]. With the aid of the expansion of σ_+, all of models are reduced to

$$\partial_\tau r(z,\tau) - \partial_z^3 r(z,\tau) = \epsilon[\partial_z^2 - \partial_z^4] r(z,\tau) + \xi(z,\tau) \tag{4·3}$$

in weakly stable region. When we start from (2·7) the scaled variables are given by $\tau = \epsilon^3 \beta t$, $z = \frac{2\zeta}{3c_0}\epsilon(x + c_0 t)$, $\xi(z,\tau) = \epsilon^3 \beta f_n(t)$ with $\epsilon = \frac{3\sqrt{c_0}}{\zeta}\sqrt{-\mu}$ and $\beta = \frac{4}{3\sqrt{c_0}}$. The solution of (4·3) is given by

$$\tilde{r}_k(\tau) \simeq \int_0^\tau ds \exp[\lambda_k(\tau - s)]\tilde{\xi}_k(s), \tag{4·4}$$

where $\lambda_k = ik^3 - \epsilon k^2(1 + k^2)$. Thus, we obtain the correlation

$$< \tilde{r}_k(\tau)\tilde{r}_{-k}(0) >= \frac{D}{2\epsilon l k^2(1+k^2)} \exp[\lambda_k \tau], \tag{4·5}$$

where l is the system size in this unit, and we use $< \tilde{\xi}_k(\tau)\tilde{\xi}_p(\tau') >= \frac{D}{l}\delta_{k+p,0}\delta(\tau - \tau')$.

Substituting (4·5) into $\phi(z,z',t) =< (r(z,t) - r(z',t))^2 >$ which is the continuous limit of the scaled ϕ_{nm}, we obtain

$$\phi(z,z',t) = 2D_G t + \frac{D}{2\epsilon l}\sum_{n\neq 0}\frac{1}{k^2(1+k^2)}\left\{|e^{ikz} - e^{ikz'}|^2 + 2(1 - e^{\lambda_k t})e^{ik(z-z')}\right\}. \tag{4·6}$$

With the aid of $\sum_{n\neq 0}\frac{1}{k^2(1+k^2)} \simeq \frac{l^2}{3} - l$ and $\sum_{n\neq 0}\frac{\cos(k(z-z'))}{k^2(1+k^2)} \simeq \frac{l^2}{3} - l|z - z'|$, the first term in the summation in eq.(4·6) is reduced to

$$\sum_{n\neq 0}\frac{|e^{ikz} - e^{ikz'}|^2}{k^2(1+k^2)} \simeq 2l|z - z'|. \tag{4·7}$$

On the other hand, the second term in the summation in eq.(4·6) becomes

$$\begin{aligned}\sum_{n\neq 0}\frac{e^{ik(z-z')}}{k^2(1+k^2)}(1 - e^{\lambda_k t}) = 2\sum_{n=1}^{\infty}\frac{\cos[k(z-z')]}{k^2(1+k^2)}\{1 - \cos(k^3 t)\} \\ +2\sum_{n=1}^{\infty}\frac{\sin[k(z-z')]}{k^2(1+k^2)}\sin(k^3 t),\end{aligned} \tag{4·8}$$

where we use the approximation $\lambda_k \sim ik^3$. Replacing the summation $\sum_{n=1}^{\infty}$ to the integral $\int_0^\infty dk$, and substituting (4·6)-(4·8) into (4·2), we obtain

$$S_k(\tau) \simeq 2\int_0^l dw \exp[-D_G k^2 \tau - \frac{Dk^2}{2\epsilon}w - \frac{Dk^2}{\pi\epsilon}\tau^{1/3}h(u)], \tag{4·9}$$

where $w = |z - z'|$, $u = x\tau^{-1/3}$, and the argument of S_k is replaced by the scaled time. D_G is the diffusion constant for the center of mass in (4·3), and $h(u)$ is

$$h(u) = \int_0^\infty dQ[\frac{\cos(Qu)}{Q^2(1 + \tau^{-2/3}Q^2)}(1 - \cos(Q^3)) + \frac{\sin(Qu)\sin(Q^3)}{Q^2(1 + \tau^{-2/3}Q^2)}], \tag{4·10}$$

where $Q^3 = k^3\tau$, and $w = |z - z'|$.

In the long time limit, eq.(4·9) is governed by the diffusion of the center of mass. For wide range of time, however, the contribution from the second and the third terms in (4·9) are dominant because of $1/\epsilon \gg 1$. In such the case, the first term is negligible, and $h(u)$ converges to

$$h(0) = \int_0^\infty dQ \frac{1-\cos(Q^3)}{Q^2} = \int_0^\infty dx \frac{\sin x}{x^{1/3}} = \frac{\pi}{\Gamma(1/3)}, \tag{4·11}$$

as time goes on. From $\lim_{l\to\infty} \int_0^l dw \exp[-Dk^2 w/(2\epsilon)] = 2\epsilon/Dk^2$, we obtain

$$S_k(\tau) \simeq \frac{4\epsilon}{Dk^2} \exp[-\frac{Dk^2}{\epsilon\Gamma(1/3)}\tau^{1/3}] \tag{4·12}$$

in intermediate time range. In the limit of small τ, $S_k(\tau) \propto 1 - \frac{Dk^2}{\epsilon\Gamma(1/3)}k^2\tau^{1/3} + \cdots$. Thus its Fourier transform, which is nothing but the power spectrum $P_k(f) =< |\tilde{\rho}_k(f)|^2 >$ obeys

$$P_k(f) \sim f^{-\alpha}, \quad \alpha = 4/3 \quad (\text{as} \quad f \to \infty), \tag{4·13}$$

where use was made of $\int_{-\infty}^{\infty} d\tau e^{i2\pi f\tau}|\tau|^{1/3} \propto f^{-4/3}$. The value 4/3 is identical to the one obtained by the experiment [11] and numerical simulations [11), 22)]. Thus our model (2·7) reproduces $\alpha = 4/3$. This result should be valid even when we start from fluid models [13), 14), 15), 16)] since the result is determined by the universal feature near the neutral curve as in (4·3). It should be noted that the appearance of this power-law form in the original model (2·7) is only for $f < \zeta$ since we eliminate the fast decaying mode σ_- in our analysis. This tendency is also observed as the higher-frequency cutoff in the experiment [11]. Thus, $f^{-4/3}$ law is determined by short time behavior of the dynamics of density waves induced by the noise, which is essentially determined by the linear dispersion relation $\lambda_k \sim ik^3$.

In this section we have confirmed the universal law $P(f) \sim f^{-4/3}$of in the frequency spectrum of density correlation function from both the simulation and the theory. We have also clarified the mechanism to emerge $f^{-4/3}$ spectrum which is related to the critical slowing down of the density fluctuations. It should be noticed that the continuous increase of α in LGA [35] from $\alpha = 0$ to 2 with the particle density is consistent with 4/3 law and our picture, because the spectrum determined by the noise in linearly stable uniform state far from the neutral curve should be white ($\alpha = 0$) and the effective exponent of the power-law becomes large when the exponential decay (i.e. $\alpha = 2$) in the off-critical region exists. There is, however, discrepancy between our results with the one on the experiment in liquids [36]. The reason of this difference should be clarified in the future.

§5. Concluding Remarks

As we have seen in section 3, our theoretical analysis gives very precise results on the phase separation between jam and non-jam phases for pure one-dimensional

models. Of course, we do not think that our analysis is perfect. Since, for example, we omit the time evolution of reduced dynamical models, we cannot explain the reason why the linearly unstable branch of the coexistence curve is stable in simulation (see Fig.1). The validity of choices of (3·18) and (3·23) are also not confirmed from mathematical point of views, although these choices work very well. To clarify the above points will be future subject of the research.

Let us comment on the universality class of traffic flows and granular flows. All of models introduced here except for (2·3) have asymmetric kink-antikink pairs and qualitatively resemble behaviors with each other. In fact, we [37] have already checked the quantitative validity of our methods presented here for the fluid model in traffic flows [13]. The results are almost identical to those explained in section 3. On the other hand, OV model in (2·3) which is a special case of the above generalized models loses some universal properties. It should be noticed that the limitation of OV model has been suggested by Komatsu and Sasa [9] (see the last part in their paper). Therefore, we believe that our analysis is meaningful to characterize universal feature of one-dimensional dissipative flows such as granular flows and traffic flows.

On the other hand, we have extended a one-dimensional deterministic model to a stochastic model supplemented by the white noise. This model clearly reproduces $P(f) \sim f^{-4/3}$ law as in the experiment [11]. We also give a simple argument for the reason why we obtain $f^{-4/3}$ law. Readers may be skeptical whether our one-dimensional models supplemented by the white noise can describe true behavior of quasi one-dimensional systems in spite of good agreement with the experiment. To reply such the question, we have already introduced a simple model for two-lanes traffic flows [38], where the vehicles have spin variable to specify what lane is chosen and lane-change of vehicles is governed by Glauber dynamics for anti-ferromagnetism. Our preliminary result of simulation also supports $f^{-4/3}$ law. Thus, $f^{-4/3}$ law is believed to be universal without regard to the choice of models. The effect of nonlinearity in the theoretical argument and the validity of the introduction of the Gaussian white noise in (2·7) will be discussed elsewhere.

In conclusion, we have proposed a simple generalized optimal velocity model (2·1). Based on the perturbation analysis of asymmetric kink solution (3·17) we obtain the selected values of its amplitude, propagating velocity and width of kink as in (3·34). The accuracy and relevancy of the solution has been confirmed by the direct simulation. We also extend a one-dimensional model to a quasi one-dimensional model with adding the white noise. From the simulation of the noise sustained model and analytic linear relaxation theory we have confirmed the universality of $f^{-4/3}$ law in power spectra in density auto-correlation function.

Acknowledgments

One of the authors (HH) thanks S. Wada, T.Takaai and O. Moriyama for fruitful discussion. This work is partially supported by Grant-in-Aid of Ministry of Education, Science and Culture of Japan (09740314).

References

[1] H.Hayakawa, H.Nishimori, S.Sasa, Y-h. Taguchi, Jpn. J. Appl. Phys. **34** (1995), 397: H.M.Jaeger, S.R.Nagel and R.B.Behringer, Rev. Mod. Phys. **68** (1996), 1259 and references therein.

[2] Y-h. Taguchi, Phys. Rev. Lett. **69** (1992), 1367: H. Hayakawa, S. Yue and D. C. Hong, Phys. Rev. Lett. **75** (1995), 2328: K. M. Aoki T. Akiyama, Y. Maki and T. Watanabe, Phys. Rev. **E54** (1996), 874.

[3] A. Rosato, K. J. Strandburg, F. Prinz and R. H. Swendsen, Phys. Rev. Lett. **58** (1987), 1038.

[4] H. K. Pak and R. P. Behringer, Nature **371** (1994), 231.

[5] F. Melo, P. B. Umbanhowar and H. L. Swinney, Phys. Rev. Lett. **75** (3838), 1995.

[6] P. B. Umbanhowar, F. Melo and H. L. Swinney, Nature **382** (1996), 793.

[7] e.g. H. Hayakawa and D. C. Hong, Phys. Rev. Lett. **78** (1997), 2764.

[8] e.g. G.B.Whitham, Linear and Nonlinear Waves (Wiley, New York, 1974); R. Huberman, Mathematical model: Traffic flow (Prentice Hall, 1977); D.Helbing, Traffic Dynamics: New Physical Modeling Concepts (Springer, Berlin, 1997).

[9] T.S.Komatsu and S.Sasa, Phys. Rev. **E52** (1995), 5574.

[10] H.Hayakawa and K. Nakanishi, patt-sol/9707003.

[11] O.Moriyama, N.Kuroiwa, and M.Matsushita, and H.Hayakawa, Phys. Rev. Lett. (to be published).

[12] M.Bando, K.Hasebe, A.Nakayama, A.Shibata and A.Sugiyama, Phys. Rev. **E51** (1995), 1035.

[13] B.S.Kerner and P.Konhauser, Phys. Rev. **E48** (1993), 2335.

[14] G.K.Batchelor, J. Fluid Mech. **193** (1988), 75.

[15] S.Sasa and H.Hayakawa, Europhys. Lett. **17** (1992), 685.

[16] T. S. Komatsu and H. Hayakawa, Phys. Lett. **183** (1993), 56.

[17] M. F. Göz, Phys. Rev. **E52** (1995), 3697.

[18] M.Doi and A. Onuki, J.Phys. (Paris) II **2** (1992), 1631.

[19] D.A.Kurtze and D.C.Hong, Phys. Rev. **E52** (1995), 218.

[20] Y.Sugiyama and H.Yamada, Phys. Rev. **E55** (1997), 7749: K. Nakanishi, K.Itoh, Y.Igarashi, and M. Bando, Phys. Rev. **E55** (1997), 6519.

[21] T.S.Komatsu, PhD thesis (Tohoku University, 1996).

[22] G. Peng and H. J. Herrmann, Phys. Rev. **E49** (1994), 1796.

[23] S. Horikawa, A. Nakahara, T. Nakayama and M. Matsushita, J. Phys. Soc. Jpn. **64** (1995), 1870.

[24] S. Horikawa, T. Isoda, T. Nakayama, A. Nakahara and M. Matsushita, Physica A **233** (1996), 699.

[25] H.Hayakawa and K.Ichiki, Phys. Rev. **E51** (1995), 3815.

[26] K. Nakanishi and H. Hayakawa, in preparation.

[27] E.J.Hinch, Perturbation Methods (Cambridge Univ. Press, Cambridge, 1991).

[28] E.Ott and R.N. Sudan, Phys. Fluids **12** (1969), 2388.

[29] Y.S. Kivshar and B. A. Malomed, Rev. Mod. Phys. **61** (1989), 763.

[30] H. Hayakawa, Teoreticheskaya i Matematicgeskaya Fizika **99**, (1994) 304.

[31] S. Ei and T.Ohta, Phys. Rev. **E50** (1994), 4672.

[32] L.Y. Chen, N. Goldenfeld, and Y. Oono, Phys. Rev. **E54** (1996), 376.

[33] In other words, the contribution from the term ρ_{41} exists if the system is under the free boundary condition [26].

[34] P.G. de Gennes, Physics **3**, (1967) 37: see also M. Doi and S. F. Edwards, *The Theory of Polymer Dynamics* (Oxford, 1986).

[35] G. Peng and H. J. Herrmann, Phys. Rev. **E51** (1995), 1745.

[36] A. Nakahara and T. Isoda, Phys. Rev. **E55** (1997), 4264.

[37] S. Wada and H. Hayakawa, J. Phys. Soc. Jpn. (to be published).

[38] T.Takaai and H.Hayakawa, in preparation.